SIMS proceedings paper

SURFACE and INTERFACE ANALYSIS

Received: 26 November 2013 Revised: 2 April 2014 Accepted: 11 April 2014 Published online in Wiley Online Library: 13 June 2014

(wileyonlinelibrary.com) DOI 10.1002/sia.5547

ToF-SIMS imaging of lipids and lipid related compounds in Drosophila brain

Nhu T. N. Phan,[a,b] John S. Fletcher,[a,b] Peter Sjövall[a,c] and Andrew G. Ewing[a,b,d]*

***Drosophila melanogaster* (fruit fly) has a relatively simple nervous system but possesses high order brain functions similar to humans. Therefore, it has been used as a common model system in biological studies, particularly drug addiction. Here, the spatial distribution of biomolecules in the brain of the fly was studied using time-of-flight SIMS. Fly brains were analyzed frozen to prevent molecular redistribution prior to analysis. Different molecules were found to distribute differently in the tissue, particularly the eye pigments, diacylglycerides, and phospholipids, and this is expected to be driven by their biological functions in the brain. Correlations in the localization of these molecules were also observed using principal components analysis of image data, and this was used to identify peaks for further analysis. Furthermore, consecutive analyses following 10 keV Ar_{2500}^+ sputtering showed that different biomolecules respond differently to Ar_{2500}^+ sputtering. Significant changes in signal intensities between consecutive analyses were observed for high mass molecules including lipids. Copyright © 2014 John Wiley & Sons, Ltd.**

Additional supporting information may be found in the online version of this article at the publisher's web-site.

Keywords: SIMS; imaging mass spectrometry; Drosophila; lipids

Introduction

Time-of-flight SIMS (ToF-SIMS) can be used as an exploratory tool to map and quantify the relative amounts of biomolecules in tissues[1–3] and cells.[4–6] In most cases, this can be carried out without extensive sample pretreatment, which is a great advantage for biological studies. Consequently, the potential of ToF-SIMS is being realized in an increasing number of biological applications.[7–9]

Drosophila melanogaster, or the fruit fly, is a well-known model system for biological studies.[10–12] The fly is small, proliferates rapidly, and has a short life cycle that is beneficial for culturing in the laboratory and collecting a large number of samples for statistical analysis. In terms of physiological effects, the fly demonstrates similarities with humans, including effects related to drug addiction making them suitable for the exploration of drug effects on the nervous system.

For brain functions, some biomolecules are known to play an important role. However, the mechanism by which these molecules change both in localization and concentration as a result of exogenous interferences, including drugs, is still not fully understood. Furthermore, many structural biomolecules, such as phospholipids, appear likely to be involved in drug action. Localization of these biomolecules is most likely related to their biological function, which has been evident in several studies.[13–16] In order to understand the mechanistic effects of exogenous interferences, it is therefore important to know the spatial distribution of the relevant biomolecular components.

In our present study, which has the principal goal to investigate chemical changes in the *Drosophila* brain following drug administration, we have used ToF-SIMS to map the localization of several biomolecules in the fly brain. In addition, the 2D molecular distribution across the fly brain after increasing amounts argon cluster (Ar_{2500}^+) sputtering was examined for 3D imaging purposes, and a variation of principal components analysis (PCA) for comparison of images is introduced.

Experimental section

Instrument

Time-of flight SIMS analysis was carried out using a J105 *3D Chemical Imager* (Ionoptika Ltd., Southampton, UK) instrument, for which details and operation principles are described elsewhere.[4,17] The instrument was equipped with a 40 kV C_{60}^+ primary ion source and a temporarily installed 10 kV Ar gas cluster ion beam (GCIB) capable of producing $Ar_{500-3500}$ clusters. In the 'static' experiments, a C_{60}^+ beam was set up to produce a beam current of approximately 10 pA with a 3 μm beam size. The analyzed area ($800 \times 800\ \mu m^2$ with 256×256 pixels, unless otherwise stated) received a primary ion dose density of 3.8×10^{12} ion/cm^2. Sputtering was performed using the Ar-GCIB, which was operated with an Ar_{2500}^+ beam current of 340 pA, delivering a cluster ion dose density of 1.91×10^{14} ions/cm^2 per sputter cycle. The sputter area was significantly larger than the analysis area to avoid edge effects. For frozen analysis, the temperature of the sample was kept below 120 K at all times.

* *Correspondence to: Andrew G. Ewing, Department of Chemical and Biological Engineering, Chalmers University of Technology, Kemivägen 10, SE-412 96 Gothenburg, Sweden.*
E-mail: andrew.ewing@chem.gu.se

a *Department of Chemistry and Molecular Biology, University of Gothenburg, Kemivägen 10, SE-412 96 Gothenburg, Sweden*

b *National Center Imaging Mass Spectrometry, Kemivägen 10, SE-412 96 Gothenburg, Sweden*

c *Chemistry, Materials and Surfaces, SP Technical Research Institute of Sweden, SE-50115 Borås, Sweden*

d *Department of Chemical and Biological Engineering, Chalmers University of Technology, Kemivägen 10, SE-412 96 Gothenburg, Sweden*

Fly culture and sample preparation

Transgenic flies tyrosine hydroxylase green fluorescent protein were cultured on potato meal/agar medium. Detailed fly culturing protocols can be found in previous literature.[18,19] Seven-day-old male flies were transferred into a 15 ml centrifuge tube, quickly frozen in liquid nitrogen and vortexed to detach the heads from the bodies. The heads were collected and then attached on the surface of a small ice cube in a plastic mold. The procedure was carried out at liquid nitrogen temperature. The fly head samples were stored in liquid nitrogen until sectioned in a cryo-microtome (Leica CM 1520, Leica Biosystems) at −20 °C under an argon atmosphere to produce 25 μm thick brain slices, which were placed onto indium tin oxide-coated microscope slides. For frozen hydrated analysis, the slides were transferred under liquid nitrogen to the J105 instrument and mounted onto a precooled sample insertion stage via an argon-filled glove box, thus minimizing the condensation of water vapor from the atmosphere. For freeze-drying, the samples were placed on a liquid nitrogen-cooled stainless steel block to slowly warm up to room temperature in a vacuum desiccator overnight. The freeze-dried samples were then transferred into the J105 instrument for analysis at room temperature.

Principal components analysis

Principal components analysis was carried out using Matlab (Version R2013a, TheMathWorks Inc., USA). The data were mean-centered, and PCA was performed using the nonlinear iterative partial least squares (NIPALS) algorithm. Individual peak selection was not performed, but multiple analyses were performed using different *m/z* ranges.

Results and discussion

Sample preparation of the fly brain

In order to extract reliable information from biological samples by ToF-SIMS imaging, it is vital that the original spatial distributions of the analyzed molecules in the samples are maintained under the vacuum conditions required for SIMS analysis. Sample preparation is therefore very important for obtaining reliable results on the chemical and spatial structures of the fly brain. Two sample preparation procedures, freeze-drying and frozen-hydrated analysis, were applied here to examine the effects of temperature on the samples. The hydrated state of the frozen sample was confirmed by the presence of water peaks in the spectra from the brain section but not from the surrounding exposed ITO substrate. The molecular distributions in freeze-dried, and frozen-hydrated fly brains were different under these two conditions. Various biomolecules, especially diacylglycerides (DAGs), distribute across the whole freeze-dried brains, whereas clear domains were observed on the frozen brains (Figure S1). For the analysis conditions used in this work, the frozen-hydrated analysis better preserved the molecular localization, whereas migration of biomolecules was observed to occur in the freeze-dried samples, presumably owing to the higher analysis temperature of the freeze-dried sample. In addition, ionization may be enhanced through the protonation by the water in the frozen-hydrated samples.[3] The frozen-hydrated method, therefore, was used for further study.

Biomolecular distribution in the fly brain

Distinct localization of biomolecules was observed in the ion images obtained from ToF-SIMS analysis of the frozen fly brain sections (Fig. 1). Strong signals arising from the phosphatidylcholine (PC) head group fragment (phosphocholine, $[C_5H_{15}NPO_4]^+$) at *m/z* 184.07 were distributed evenly across the brain. PC is the main lipid component of the cell membrane; therefore, its strong homogeneous signal is a good indication of insignificant topography. Several low mass peaks were observed only in the optical lobes, such as *m/z* 230.11, 369.14, and 370.15. Interestingly, the peak with *m/z* 369.14 is not attributed to cholesterol (commonly observed at *m/z* 369.35 $[M+H-H_2O]^+$ on cell and tissue samples analyzed with ToF-SIMS) as the other major cholesterol peaks such as 385.35 $[M-H]^+$, 753.74 $[2M-H_3O]^+$ are not present in the spectra.[20] The mass resolution of the instrument clearly distinguishes mass *m/z* 369.14 from *m/z* 369.35. Instead, this peak is assigned to the red eye pigment, drosopterin ($C_{15}H_{16}O_2N_{10}$), which has been shown to produce the molecular ion at *m/z* 369.15 in liquid chromatography Fourier transform mass spectrometry analysis of *Drosophila*.[21,22] In addition, the salt adducts with sodium at *m/z* 391.14 and potassium at *m/z* 407.10 were also observed, which confirms the drosopterin assignment. The other peaks localizing in the optical lobes are also expected to originate from the eye pigments; however, this has not yet been confirmed.

Signals of DAGs with different numbers of carbon atoms, from C_{12} to C_{18}, and double bonds in the two fatty acid chains were found in the center area of the brain. DAGs can originate from the fragmentation of triacylglycerides or can be derived from the hydrolysis of phospholipids. DAGs have been known as important secondary messengers for cell growth and other cellular functions.[23] The overlay image of DAGs and the PC fragment at *m/z* 184.07 shows no colocalization in the tissue, thus indicating that phosphocholine-containing lipids are not the main source for DAGs. In addition, signals from other peaks are distributed over the whole brain area, particularly *m/z* 152.05 and 153.04. With the mass accuracy of 25 ppm, these peaks are not hydrocarbon fragments but are tentatively assigned to guanine and xanthine, which are found in the metabolomic profile of *Drosophila*.[22,24]

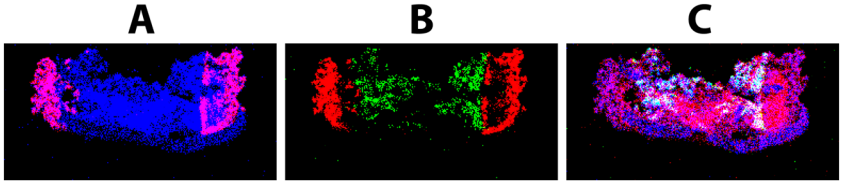

Figure 1. Localization overlay of different biomolecules in a frozen fly brain analyzed with the C_{60}^+ ion source, positive mode. A. PC fragment *m/z* 184.07 (blue) and eye pigment drosopterin *m/z* 369.14 (red). B. *m/z* 230.11 (red) and DAG (28 : 0) *m/z* 495.44 (green). C. PC fragment *m/z* 184.07 (red), DAG (30 : 1) *m/z* 521.46 (green), and *m/z* 152.05 (blue). The analyzed area is $400 \times 800\ \mu m^2$ with 128×256 pixels receives a primary ion dose density of 3.8×10^{12} ion/cm^2.

SURFACE and INTERFACE ANALYSIS

Exploration of molecular distribution changes by image principal components analysis

The application of multivariate analysis methods, such as PCA, to ToF-SIMS data has become increasingly common and has been widely used for classification of various chemicals or biological specimen, image contrast enhancement and for facilitating realistic 3D visualization.[25–28]

Principal components analysis identifies the largest variance between groups of samples on the basis of the variables associated with the sample. In the case of ToF-SIMS data, the samples are mass spectra, and the variables are *m/z* values. A series of principal components (PCs) are calculated, where PC1 captures the largest variance between the samples, PC2 the second largest variance, and so on. Each PC has a loading (eigenvector), which explains what variables are contributing to the variance captured by that PC. Samples are given a score (eigenvalue) against the loading. Samples with the same amount of variance related to a specific PC will have the same score. When applied to ToF-SIMS images, the samples are spectra and each spectrum corresponds to a different pixel. By mapping the score values onto a suitable color scale, score images can be generated. This provides a useful method for visualizing differences (and similarities) between pixels (and therefore spectra that reflect chemical composition) in the image.

Principal components analysis is normally applied to a single ToF-SIMS image to look for differences within the image. Here, we took a novel approach. We used PCA to investigate the changes of different chemistries in a series of images. The data from three images acquired after increasing bombardment with 10 keV Ar_{2500}^+ were combined in Matlab (concatenation). PCA was then performed on the spectra from all three images at once so that 'between image' variation could be assessed.

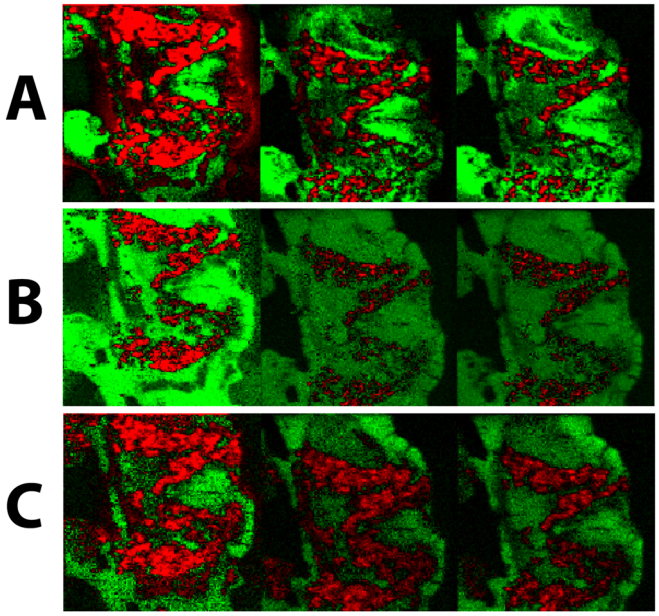

Figure 2. Image PCA to compare molecular distribution on a fly brain from three consecutive analyses with a C_{60}^+ ion source and sputter with Ar_{2500}^+ 10 KeV in between, positive mode. From left to right are the first, second, and third layers. A. Selecting the *m/z* 120–900 range; PC 4 shows DAG (26 : 0) *m/z* 467.41, DAG (28 : 0) *m/z* 495.44, and DAG (30 : 1) *m/z* 521.46 localize in the red area; and dominant peaks at *m/z* 213.15, 197.16, drosopterin *m/z* 369.14 localize in the green area. B. Selecting the *m/z* 460–670 range; PC 2 shows DAG (26 : 0) *m/z* 467.41, DAG (28 : 0) *m/z* 495.44, and DAG (30 : 1) *m/z* 521.46, DAG (30 : 0) *m/z* 523.47 localize in the red area; dominant peaks at *m/z* 576.55, 571.41, 604.54 localize in the green area. C. Selecting the *m/z* 670–900 range; PC 4 shows dominant peaks at *m/z* 702.41, 771.63, PC (36 : 2) at *m/z* 786.60 localize in the red area; and *m/z* 671.46, PC (34 : 1) *m/z* 760.61 localize in the green area.

Molecular information might change in consecutive analyses with Ar sputtering

Acknowledging the benefits from image PCA, we applied the method to investigate the change in chemical distribution across a fly brain with repeated analyses using C_{60}^+ accompanied by Ar_{2500}^+ sputtering. The frozen sample was first analyzed using C_{60}^+ to produce an ion image, then sputtered by Ar_{2500}^+ with a dose of 1.91×10^{14} ions/cm^2 per sputter cycle. The image of the second layer was obtained after sputtering, and the procedure was repeated several times. Three C_{60}^+ ion images were combined for analysis using image PCA (Fig. 2). Pixels are displayed on a red/black/green color scale where negatively scoring pixels are red, positive are green, and the pixels showing zero variance on the selected PC are black.

Three mass ranges were selected to highlight the variation between different chemical species. The widest mass range included all the *m/z* channels between *m/z* 120 and *m/z* 900. Starting at *m/z* 120 avoided the extremely intense In^+ signal from the substrate surrounding the sample. The second mass range used was *m/z* 460–670 focusing on the signals arising from the DAGs, and the final mass range selected was *m/z* 670–900, where signals of intact phospholipid and triacylglycerides species occur.

For the widest mass range, *m/z* 120–900 (Fig. 2A), it was shown in PC 4 that the DAGs, particularly DAG (26 : 0) at *m/z* 467.41, (28 : 0) at *m/z* 495.44, and (30 : 1) at *m/z* 521.46, localized to the middle brain area. Strong signals were observed at the first layer relative to other peaks such as those from the eye pigments. The localization of these DAGs and small molecules, which colocalize with DAGs, was significantly different after Ar_{2500}^+ etching. It could be that small molecules delocalize on the brain surface, therefore their distribution is clearer after removing the top layer. Other possible explanations might be that these peaks originate from the cuticles, which might remain on top of the brain after sectioning with the cryo-microtome or that a small amount of smearing might have occurred during slicing or thaw mounting.

Considering only the mass range *m/z* 460–670 for the DAGs (Fig. 2B), significant differences between these and other as yet unidentified peaks were observed in PC 2. The localization of the DAGs does not change considerably between the three layers; however, the intensities of DAG signals decrease slightly after Ar_{2500}^+ etching.

Because of low intensities for the lipid molecular ion peaks compared with other smaller molecules, their contribution to spectral variations is not easily observed. PCA can, however, be used to highlight the variations when performed for high mass range $m/z > 670$ (Fig. 2C). Interestingly, several unidentified peaks are found to localize in correlation with the DAGs. These include *m/z* 702.41, 771.63, and PC (36 : 2) at *m/z* 786.60, whereas *m/z* 671.46 and PC (34 : 1) at *m/z* 760.61 localize in different areas. This provides further evidence for the argument previously discussed that the DAGs observed do not mainly originate from phosphocholine containing lipids. With image PCA, the correlation in distribution between different molecular groups is convincingly presented despite their relatively large difference in signal intensities. In contrast to the small molecules, which

appear to delocalize on the sample surface during sample preparation, the distribution of high mass molecules is unchanged after Ar_{2500}^+ etching. However, the signal intensities of intact lipid species decrease significantly in the second and third layers. These experiments were repeated on different brain slices to check reproducibility. Molecules have been shown to be affected by Ar_{2500}^+ cluster sputtering differently, especially high mass molecules such as lipids. To avoid interferences from the surrounding environment and artifacts from sample preparation, which usually occur on the very top layer of samples, it is advantageous to carry out analysis after sputtering the top layer with the Ar-GCIB. However, it should be noted that different molecules respond differently to the sputtering.

Conclusions

In this paper, we introduce a new biological application for SIMS, imaging of *Drosophila* brain for the study of drug interactions with brain chemistry and structure. A sample preparation protocol for this extremely small sample has been successfully developed. Frozen analysis methodology is shown to preserve the chemical and spatial information of the fly brain. Different spatial distributions of several biomolecules are observed, apparently related to their biological functions in specific brain regions. For data analysis, a new variant of image PCA using the entire spectra instead of individual mass peaks from several MS images at once has been shown to be very useful to identify changes in the distribution of biomolecules. Sputtering with the Ar-GCIB has been used to remove smearing defects from the sample surface to obtain more reliable chemical information; however, it appears that the Ar cluster sputtering might affect the intensity of high mass molecules. Consecutive analyses with Ar_{2500}^+ sputtering or 3D imaging, therefore, should receive careful consideration to avoid discrimination between different molecules. ToF-SIMS will be further applied to the fly brain model to study chemical effects of the stimulant drug, methylphenidate, on lipids and lipid-related molecules.

Acknowledgements

The authors acknowledge grants from The European Research Council (ERC), Knut and Alice Wallenberg Foundation, the Swedish Research Council (VR), and the National Institutes of Health.

References

[1] P. Sjövall, B. Johansson, D. Belazi, P. Stenvinkel, B. Lindholm, J. Lausmaa and M. Schalling, *Appl. Surf. Sci.* **2008**, *255*, 1177.
[2] D. Debois, M. P. Bralet, F. Le Naour, A. Brunelle and O. Laprevote, *Anal. Chem.* **2009**, *81*, 2823.
[3] T. P. Roddy, D. M. Cannon, S. G. Ostrowski, A. G. Ewing, N. Winograd, *Anal. Chem.* **2003**, *75*, 4087.
[4] J. F. Fletcher, S. Rabbani, A. Henderson, P. Blenkinsopp, S. P. Thompson, N. P. Lockyer, J. C. Vickerman, *Anal. Chem.* **2008**, *80*, 9058.
[5] I. Lanekoff, M. E. Kurczy, K. L. Adams, J. Malm, R. Karlsson, P. Sjövall and A. G. Ewing, *Surf. Interface Anal.* **2011**, *43*, 257.
[6] M. E. Kurczy, P. D. Piehowski, C. T. Van Bell, M. L. Heien, N. Winograd and A. G. Ewing, *Proc. Natl. Acad. Sci. U. S. A.* **2010**, *107*, 2751.
[7] K. R. Tucker, Z. Li, S. S. Rubakhin, J. V. Sweedler, *J. Am. Soc. Mass Spectrom.* **2012**, *23*, 1931.
[8] J. S. Fletcher, J. C. Vickerman, *Anal. Chem.* **2013**, *85*, 610.
[9] M. L. Steinhauser, A. P. Bailey, S. E. Senyo, C. Guillermier, T. S. Perlstein, A. P. Gould, R. T. Lee, C. P. Lechene, *Nature* **2012**, *481*, 516.
[10] S. C. Piyankarage, D. E. Featherstone, S. A. Shippy, *Anal. Chem.* **2012**, *84*, 4460.
[11] E. C. Berglund, M. A. Makos, J. D. Keighron, N. Phan, M. L. Heien, A. G. Ewing, *ACS Chem. Neurosci.* **2013**, *4*, 566.
[12] U. B. Pandey, C. D. Nichols, *Pharmacol. Rev.* **2011**, *63*, 411.
[13] N. D. Volkow, G. Wang, J. S. Fowler, J. Logan, B. Angrist, R. Hitzemann, J. Lieberman, N. Pappas, *Am. J. Psychiatry* **1997**, *154*, 50.
[14] G. Charach, N. Kaysar, I. Grosskopf, A. Rabinovich, M. Weintraub, *J. Clin. Pharmacol.* **2009**, *49*, 848.
[15] F. Schmitz, E. B. Scherer, F. R. Machado, A. A. da Cunha, B. Tagliari, C. A. Netto, A. T. Wyse, *Metab. Brain Dis.* **2012**, *27*, 605.
[16] N. D. Volkow, G. Wang, Y. Ma, J. S. Fowler, W. Zhu, L. Maynard, F. Telang, P. Vaska, Y. Ding, C. Wong and J. C. Swanson, *J. Neurosci.* **2003**, *36*, 11461.
[17] R. Hill, P. Blenkinsopp, S. Thompson, J. Vickerman, J. S. Fletcher, *Surf. Interface Anal.* **2011**, *43*, 506.
[18] N. J. Kuklinski, E. C. Berglund, J. Engelbrektsson, A. E. Ewing, *Anal. Chem.* **2010**, *82*, 7729.
[19] N. T. Phan, J. Hanrieder, E. C. Berglund, A. G. Ewing, *Anal. Chem.* **2013**, *85*, 8448.
[20] P. Sjovall, J. Lausmaa and B. Johansson, *Anal. Chem.* **2004**, *76*, 4271.
[21] H. Kim, K. Kim, J. Yim, *IUBMB Life* **2013**, *65*, 334.
[22] M. A. Kamleh, Y. Hobani, J. A. Dow, L. Zheng, D. G. Watson, *FEBS J.* **2009**, *276*, 6798.
[23] Y. Nishizuka, *FASEB J.* **1995**, *9*, 484.
[24] M. A. Kamleh, Y. Hobani, J. A. Dow, D. G. Watson, *FEBS Lett.* **2008**, *582*, 2916.
[25] D. J. Graham, M. S. Wagner, D. G. Castner, *Appl. Surf. Sci.* **2006**, *252*, 6860.
[26] O. D. Sanni, M. S. Wagner, D. Briggs, D. G. Castner, J. C. Vickerman, *Surf. Interface Anal.* **2002**, *33*, 715.
[27] B. Vaezian, C. R. Anderton, M. L. Kraft, *Anal. Chem.* **2010**, *82*, 10006.
[28] J. S. Fletcher, S. Rabbani, A. Henderson, N. P. Lockyer, J. C. Vickerman, *Rapid Commun. Mass Spectrom.* **2011**, *25*, 925.

Supporting information

Additional supporting information may be found in the online version of this article at the publisher's web-site.